Bioelectrochemistry 146 (2022) 108138

Contents lists available at ScienceDirect

Bioelectrochemistry

journal homepage: www.journals.elsevier.com/bioelectrochemistry

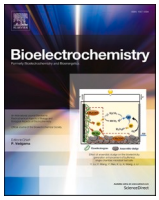

Nonlinear electric response of the diffuse double layer to an abrupt charge displacement inside a biological membrane

Hamdy I.A. Mostafa [a,b], Rudolf Tóth-Boconádi [a,1], László Dér [a], László Fábián [c], Stefka G. Taneva [d], András Dér [a,*], Lajos Keszthelyi [a,*]

[a] Institute of Biophysics, Biological Research Centre of Eötvös Loránd Research Network, H-6701 Szeged, Hungary
[b] Biophysics Department, Faculty of Science, University of Cairo, Giza 11757, Egypt
[c] Department of Experimental Physics, University of Szeged, H-6725, Szeged, Dóm tér 9, Hungary
[d] Institute of Biophysics and Biomedical Engineering, Bulgarian Academy of Sciences, 1113 Sofia, Bulgaria

ARTICLE INFO

Keywords:
Charge separation
Bacteriorhodopsin
Purple membrane
Nonlinear response

ABSTRACT

In order to elucidate the old, still unsolved problem of how the diffuse electric double layer responds to an abrupt, intramolecular charge displacement inside a biological membrane, we investigated the fastest components of the light-induced electric signals of bacteriorhodopsin and its mutants, in numerous ionic and buffer solutions. The obtained data for temperature and solute concentration dependence were interpreted as a consequence of changes in the capacity of the diffuse double layer surrounding the purple membrane. The possible physiological consequences of this so far not demonstrated phenomenon are discussed.

1. Introduction

Recent advances in membrane electrophysiology research have repeatedly called the attention to the importance of the immediate consequences of intramembraneous charge rearrangements in, e.g., biological signal- or energy transduction processes [1]. Given the know-how piled up in our lab during the past decades in developing new methods for the measurement of electric signals of ion-pumping membrane proteins [2–5], we addressed this problem by detecting electric signals induced by the ultrafast primary charge separation events in bacteriorhodopsin (BR), the paradigmatic proton pumping protein.

BR molecules are embedded in the cell membrane of *Halobacterium salinarum,* and concentrated in purple membrane patches (*pm*). They undergo a cyclic photoreaction upon light excitation, and transport one proton per cycle from the cytoplasm of the bacterium to the medium. Methods were worked out to observe the electric responses due to the movements of charges inside BR molecules [2]. Shortly: *pm* oriented in suspension is illuminated with appropriate laser flash, and the arising well-measurable electric signal is recorded. Among the multitude of components, the fastest one is of negative sign (related to the direction of proton transport). The time resolution of the obtained signal depends on the length of the laser flash, and on the measuring system. In carefully accomplished experiments carried out by picosecond laser-pulse excitations on dried, oriented pm samples, a single negative component was registered on the picosecond time scale [6,7]. In *pm* oriented in solution or in gel, however, the fast negative signal revealed two rising components: one that followed the length of the laser flash (τ_1 component) and one that increased it but its time behaviour depended on the resistance and temperature of the solution (τ_2 component) [5]. This second component was assigned to charge motion in the diffuse double layer around *pm*. After these two rising components, the signal decays with an exponential of life time τ_3 due to the measuring system. This fast electric signal is followed with further components related to the charge motion in the photocycle of BR as discussed in [2,8].

Unsolved problems still remained: a) what is the real role of the diffuse double layer in the genesis of the fast components, b) what is the process which determines the amplitude ratio of the two rising components. In order to approach these questions, the temperature and ionic concentration dependence of the fast components of the bR electric signal were studied in cases of different BR mutants. The results summarized in the present study confirmed and broadened the previous experimental findings, and were interpreted according to changes in the capacity of the diffuse double layer around *pm*. Since, similarly to bR, most of the ion pumps are assumed to transport charges across the cell

* Corresponding authors.
E-mail address: keszthelyi.lajos@brc.hu (L. Keszthelyi).
[1] Deceased.

https://doi.org/10.1016/j.bioelechem.2022.108138
Received 24 January 2022; Received in revised form 15 April 2022; Accepted 20 April 2022
Available online 23 April 2022

membrane via a series of abrupt conformational transitions [3,8], such an effect on the diffuse double layer may well have general physiological implications that are shortly discussed in the paper.

2. Materials and methods

Purple membranes separated from wild type bacteriorhodopsin (WTBR), and double-mutant strains D96N/D115N and R82Q/D85N (expressed in *Halobacterium salinarum* strain L-33) were used in the present investigations. The samples were supplied by Prof. J. K. Lanyi, in form of *pm* fragments. The fragments were washed three times in tri-distilled water, and gently sonicated for 5 *s*, to remove the aggregated parts, prior to preparation for measurements.

After these treatments, the *pm*-s were oriented and immobilized in a polyacrylamide gel [4]. (Note that in the original version of the suspension method, measurements were performed in solutions, during the orienting field was applied [2], but above ionic strengths of a few mM, the orientation of the membrane fragments is not feasible, due to electrostatic screening of their permanent dipole moment [9]. Hence, at low ionic strength, the orientation of membrane fragments is fixed in gel [10], which can then be penetrated by the desired solution of arbitrary concentration [4].) The gel was cut into pieces each of 6 × 4 × 12 mm and washed in tridistilled water several times. Pieces that trapped air bubbles or were inhomogeneous in their optical density were excluded. The gels slabs were immersed into a 40 × 4 × 14 mm measuring cuvette encased in a copper Faraday cage, with a hole of 20 mm^2 for light excitation, while 20 × 4 mm platinized electrodes inserted in the cuvette picked up the electric signals.

Before measurements, the gels were equilibrated with the appropriate solutes, at least overnight. The pH of the solutions was measured at the time of the experiment. Cations of increasing valence (Na^+, Ca^{++}, V^{+++}), with the same anion (Cl^-), and in the case of Na^+ with different anions (phosphate and bicarbonate), were used for equilibration. Two types of buffers, glycil-glycine (GLY-GLY) and *bis–tris* propane (BTP) were also used to elucidate the effect of buffers of different charge and pK on the two components of the first electric signal in WTBR.

The pH was set to 7 for all equilibrated solutions, except for the case of buffers (pH 6 and 7 for GLY-GLY, 7 and 9.5 for BTP). The temperature was set with a thermostate in the range of 2C– to 35C.

The samples were flashed with the light of a dye laser (rhodamine 6G) excited with an excimer laser (Lambda Physik EMG 101 MSC, Göttingen, Germany) at 580 nm, 20 ns duration and 2 mJ energy. The arising signals were collected with a home-made FET follower, and transferred to an IWATSU TS 8123 digital oscilloscope, with a rise time of 3 *ns*. Exponential fitting of the traces was performed by the computer program, Origin 8.1 (OriginLab Co.). Electric substitution-circuit-wise simulation of the voltage response of the membrane-electrolyte system to an abrupt charge displacement in the protein was carried out by the software Matlab-Simulink R2018b (MathWorks Inc.).

3. Results

a) Wild-type bacteriorhodopsin

Signals from single-shot excitations of short (nanoseconds) laser flashes were recorded at different temperatures (2–35 °C), and different ionic and buffer environments. The signals shown in Fig. 1 were recorded on a WTBR gel sample immersed into 5 mM NaCl solution at 7 different temperatures (for easier observation, only two traces are shown). All traces start with a fast, $\tau_1 = 20$ *ns* (10–90%) rise-time component. The duration of this component was determined by the length of the laser flash, independent from the temperature. The rise of the negative signal was completed with an exponential growth of life time τ_2. After reaching its maximum absolute value, the signal decayed with life time of τ_3. We note here that at higher temperatures two more components appear on the recorded time scale, belonging to the K-L and

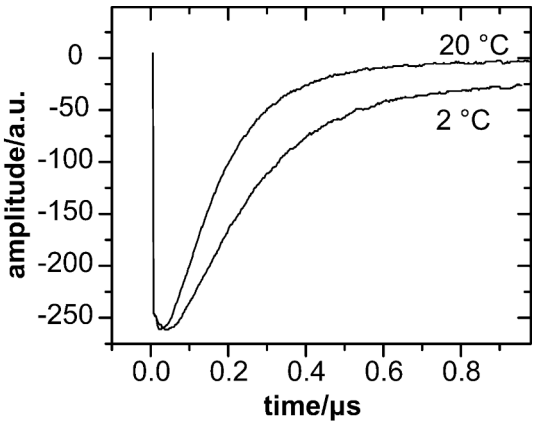

Fig. 1. Temperature dependence of the first fast electric signal in case of wild-type bacteriorhodopsin in 5-mM NaCl solution (for easier observation, only two traces are shown).

L-M transitions of the photocycle. All the traces recorded at different temperatures were fitted with exponentials.

Based on this evaluation, we demonstrate the exponential-decomposition structure of the first three components that determine the time evolution of the electric signal after laser excitation (Fig. 2). The fastest component levels off at amplitude A_1 (a negative value) with life time τ_1, while the second component (with amplitude A_2 (<0) and life time τ_2) further increases the absolute value of the signal until it is cut off by the decay component determined by the life time of the measuring system (τ_3).

To acquire more information about the processes, the dependence of A_1/A_2, τ_2 and τ_3 on temperature (T) and on the solutions were determined under various conditions.

In the first series of experiments, mono-, di-, and tri-valent cations, Na^+, Ca^{++} and V^{+++} with Cl^- anions were used to check whether the valence has any effect on A_1/A_2 and τ_3/τ_2. In the next series, the Cl^- anions were exchanged to phosphate and bicarbonate anions. Further on, GLY-GLY and BTP buffers were added to the bathing solution at two pHs (6 and 7 for GLY-GLY and 7 and 9.5 for BTP). Amplitude and time constant ratios at different temperatures were determined for these cases, too. Figs. 3 and 4 show that they remained constant, with averages $A_1/A_2 = 0.578(15)$ and $\tau_3/\tau_2 = 4.01(67)$. (We note that the data for buffers somewhat scatter due to changes in protonation with temperature.).

From the constancy of τ_3/τ_2, it may be stated that change of both life times is determined similarly with the changing resistance due to the changing temperature. From the temperature-dependence of τ_2 and τ_3, recorded for all cases, Arrhenius plots were constructed. The data of

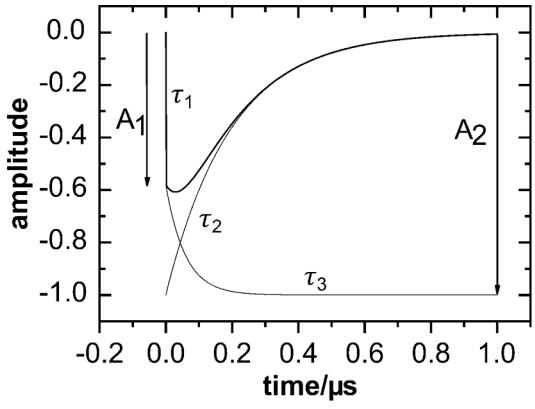

Fig. 2. Representation of the exponential decomposition of the first electric signal (explanation in the text).

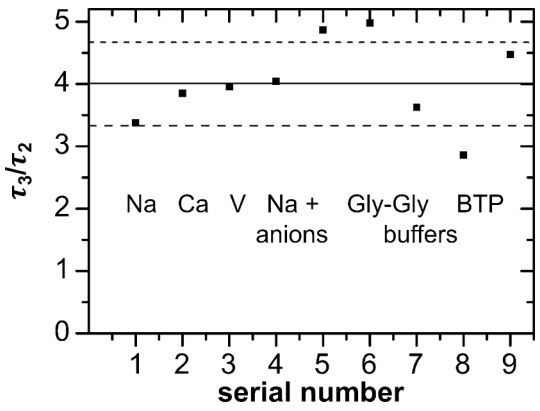

Fig. 3. τ3/τ2 values for signals of wild-type bacteriorhodopsin oriented in gel, soaked in 5-mM ionic and buffer solutions. For the buffers, the measurements were done at 2 different pH values, specified in Table 2, depicted in increasing order. The average value is: $\tau_3/\tau_2 = 4.01$ (67).

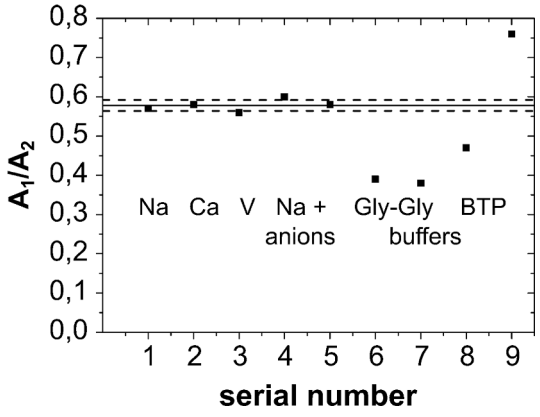

Fig. 4. A_1/A_2 values for ionic and buffer solutions. 5 mM wild type bacteriorhodopsin oriented in gel. For the buffers, the measurements were done at 2 different pH values, specified in Table 2, depicted in increasing order. The average value is 0.578 (15).

activation enthalpies for ionic solutions are summarized in Table 1, for buffers in Table 2. The average values for $\tau_2 = 12.9(8)$ for τ_3 14.1(1.4) kJ/mol^{-1}, thus equal within error.

The average values in the case of the buffers are 17.3 (1.2) and 17.87 (1.9) kJ·mol^{-1} for τ_2 and τ_3 respectively. The activation enthalpy values may be calculated for the resistances of ionic solutions from data in Handbook of Chemistry and Physics [11]. The value for NaCl is 15.9 (1) kJ·mol^{-1}. Thus, it may be confirmed that the measured activation enthalpies for the ionic and buffer solutions are in the range of the activation enthalpies for resistances of ionic solutions. Consequently, we attribute the temperature dependence of τ_2 and τ_3 to the alteration of resistances and the temperature-independent capacitances. The ionic concentration dependence of the A_1/A_2 values is shown in Figs. S3-S5. These data support that the signals originate from the diffuse double layers (see Eq. (1)).

Table 1
Activation enthalpies for the electric signal components of life times τ_2 and τ_3 in different ionic solutions. The signals were measured on wild-type bacteriorhodopsin oriented in gel, soaked in 5-mM solutions of the listed salts.

Solutes	Activation emthalpy for τ_2 (kJ·mol^{-1})	Activation emthalpy for τ3 (kJ·mol^{-1})
NaCl	14.11 (1.56)	12.62 (98)
$CaCl_2$	12.02 (1.56)	16.96 (312)
VCl_3	12.75 (2.11)	1337 (32)
Na-phosphate	12.43 (2.22)	16.5 (1.2)
Na-bicarbonate	12.82 (1.32)	14.2 (1.1)

Table 2
Activation enthalpies for the electric signal components of life times τ_2 and τ_3. The signals were measured on wild-type bacteriorhodopsin oriented in gel, soaked in various buffer solutions of 5-mM concentration.

Buffers	Activation emthalpy for τ_2 (kJ·mol^{-1})	Activation emthalpy for τ_3 (kJ·mol^{-1})
Gly-GlY pH 6	17,45 (312)	
Gly-GLY pH 7	16.33 (72)	16.6 (7)
Bis-Tris Propane pH 7	18.8 (2.7)	16.0 (2.0)
Bis-Tris Propane pH 9.5	16.6 (4.3)	17.9 (2.0)

b) bacteriorhodopsin mutants

The parameters of the fast electric signal for two double mutants of bacteriorhodopsin which do not pump protons, are shown in Figs. S1 and S2, for D96N/D115N BR and R82Q/D85N BR, respectively. The dominant, temperature-dependent τ_2 component is missing in these cases, instead, we observe a short-time decrease and increase, respectively, before the decrease due to the temperature-dependent decay of the τ_3 component. The temperature-dependence of these short-living components could not be determined.

4. Discussion

The results of the electric signal measurements can be summarized as follows:

1) The second and third components of the fast electric signal in flash excitation of bacteriorhodopsins (wild type and mutants) appear for all ionic and buffer solutions applied.
2) Their duration is in the order of 10 to100-nanoseconds.
3) The temperature dependence of these components differs from that of any BR photocycle components, and the activation enthalpies are in the range of those of the conductivities of ionic solutions.
4) They are much shorter and smaller for double mutants.
5) The amplitude ratio A_1/A_2 decreases with the increase of the ionic concentration of the solution.

We think that all these findings can be understood based on the following hypothesis: the light-induced electric signal, caused by charge displacements inside the bR molecules embedded in purple membranes, propagates through the diffuse double layer around the membrane and thought the solution, hence, both of them influencing it. The fast, negative component is due to the primary events of the bR photocycle in the subpicosecond to picosecond range, reflecting charge displacements opposite to the overall direction of proton pumping [2]. It appears as an abrupt rise of a "negative" signal on this time scale (the first component following the short light-flash), that is limited by the time resolution of the measuring circuit (preamplifier and oscilloscope). The subsequent movement of charges in the double layer and the solution is reflected in the second and third components of the electric signal, respectively.

Here, we should emphasize that, in the absence of nonlinear effects, the voltage change in the far-field due to an abrupt charge separation inside the membrane is supposed to follow by a subsequent unidirectional relaxation due to the rearrangement of ions around the membrane fragment, eventually leading to a complete screening of the dipole, as it has been underpinned by our Brownian-dynamics simulation results [12]. From this viewpoint, the bipolar relaxation observed in our experiments is an intriguing phenomenon, implying the occurrence of nonlinear effects.

Considering the conventional electric substitution circuit models for the diffuse double layer (Scheme 1), we can associate a capacitance C_{dl} to the double layer, and the shortcut-resistance around the membrane R_{SC}. The thickness of the double layer is considered to be.

$$d = (ee_o k_B T/2e^2 n)^{1/2}, \quad (1)$$

where ε and ε_o are the dielectric constant and the vacuum permittivity, respectively, k_B the Boltzman constant, T the absolute temperature, n the ion concentration, and e the elementary charge. For the whole sample, where oriented purple membrane fragments are suspended in the electrolyte, C_{DL} and d are connected with a simple equation.

$$C = ee_o A/d \quad (2)$$

where A is the sum of all individual oriented purple membrane surface areas in the sample. R_{SC} is the resulting resistance of the parallelly connected individual resistors. While the individual values sum up for C_{dl} increasing it, R_{SC} gets smaller due to the simple Ohm's law.

The capacitance and resistance of the solution and the measuring system are C_2 and R_2, respectively (Fig. S7). The membrane capacitance, C_m, the double-layer capacitance, C_{dl} and the electrode capacitance C_2 are switched in a serial circle (Fig. S7).

Because d inversely depends on the square root of ionic concentration (n in Eq. (1)), C_{dl} depends directly on it (Eqs. (1) and (2)).

An intramembraneous charge displacement can be characterized by an electric dipole moment change, whose electric field is considerably delocalized to a larger area of the membrane (see the well-known, 515-nm carotenoid absorption shift in chloroplast [13], and its interpretation by electrostatic calculations [14].) This extensive change in the electric field should, in turn change the surface potential (ψ) of the membrane, as well, that may eventually result in release or uptake of ions by the membrane surface to or from the solution. The subsequent change of ion concentration in the diffuse double layer should change its capacity (C_{dl}), as well. The surface-potential dependence of the double-layer capacity is the reason why the notion of differential capacitance ($C_d = d\sigma/d\psi$, where σ is the surface charge density of the membrane) is widely used in attempts to characterize the electric behaviour of diffuse double layers [15,16], always bearing in mind that a simple substitution circuit model gives a rather qualitative than quantitative description of the electric properties of a complex, distributed-parametric system.

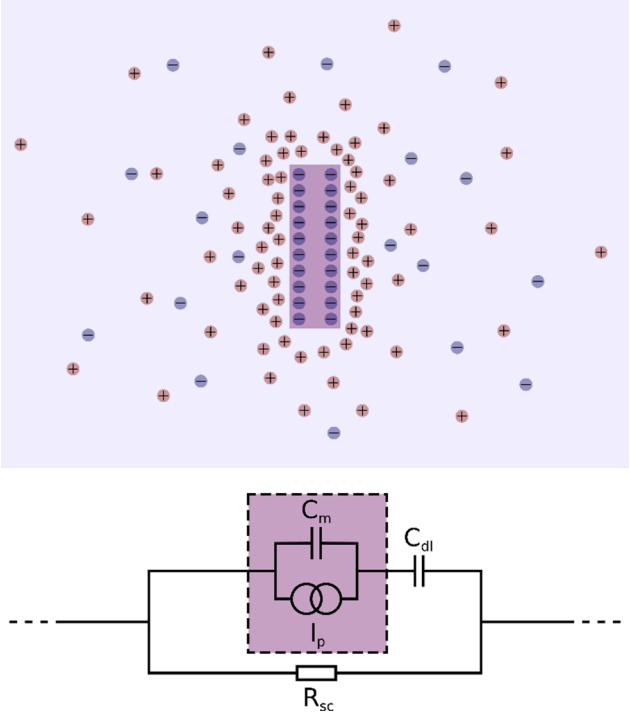

Scheme 1. Above, the schematic representation of the purple-membrane - electrolyte system, with fixed negative surface charges on the membrane, and the diffuse electric double layer in the vicinity of it. Below, the substitution electric circuit used in our simulations to model the electric behaviour of the membrane – double-layer system. I_p is the current generator representing the synchronous action of the bR pump proteins in the sample (resulting in charge displacements within the membrane, and a subsequent rearrangement in the double layer), C_m and C_{dl} are the capacitances associated to the purple membranes and the surrounding double layers, respectively, while R_{SC} stands for the short-cut resistance around the membranes in the sample.

Hence, to qualitatively interpret our experimental results, we follow the above arguments, and assume that the electric capacity of the double layer changes, due to the internal charge motion following the laser flash that triggers synchronized charge displacements in the bR molecules in the sample.

The motion of charges in the double layer takes time determined with the mobility of the ions [17]. This way the C_{dl} component should control the time behaviour of the second component of the electric signal. The similarity of the activation enthalpies to those of the conductivity shows that the mobility of ions in the double layer is the same as in the solution. When comparing ionic mobilities, one should bear in mind that our measurements were performed in polyacrylamide gels, due to technical reasons (see Materials and Methods). According to our earlier experiments [3,4], however, the kinetics of the components of bR electric signals (including the fastest one), is not influenced by the presence of the gel to a measurable extent. The gel is a relatively sparse and flexible network of a pore size of several nanometers [18], considerably larger than the hydrodynamic radius of the cations and anions used in our experiments, and their mean free path in water. More recent results of independent experiments on the comparison of ionic mobilities in 15%-w/w polyacryalamide gels and gel-free solutions show that above ionic strengths of 1 mM, the two conductivities do not differ more than 5% [19]. Since in our case the gel concentration was only 7.5%, one can reasonably assume that the influence of the gel on the calculated activation enthalpies remained within the error limits of the measurements coming from other experimental uncertainties. The smallness of the second component in cases of double mutants indicates that the influence of internal charge motion is largely compensated with the doubly changed internal ionic distribution in BR, resulting in an impaired charge displacement, and hence, inducing a disproportionately smaller nonlinear response of the double layer. With increasing ionic concentration, the thickness of the double layer decreases (Eq. (1)), consequently its modification due to internal charge motion decreases too increasing C_{dl} with the square-root of the concentration while decreasing R_{SC} linearly with it, resulting in $R_{SC}{\cdot}C_{dl}$ decreasing with the square root of the concentration. As a consequence, the same charge yields smaller voltage on the electrodes, as seen in Figs. S3-S6.

In order to check whether a simple electric substitution circuit model of the combination of the membrane-bound proton pump and the electrolyte – measuring-electrode system can account for the above phenomenology, model calculations were performed. The equivalent circuit of the system was a modified version of the one used to describe the electric response of the purple membrane - electric double-layer system [20], complemented by an RC part for the surrounding electrolyte (Fig. S7). Light-excitation of the sample initiates synchronous charge displacements inside the bR pump-proteins, that, in turn, cause a displacement current charging the membrane capacitance, and it is taken into account as a current generator in the equivalent circuit (Scheme. 1 and Fig. S7). Here, we made use of the results of our earlier experiments and Brown-dynamics simulations that are consistent with a response time of the electric double-layer system to an abrupt intramembrane charge displacement falls in the100-ns range. The perturbation caused by this current pulse is by subsequent relaxation processes, determined by the resistances and capacitances of the system. The magnitude of their values used in the simulations were congruent with earlier experimental data [21,20] and theoretical treatments of the

dynamics of the diffuse double layer [17,22]. The results of the calculations showed that there is an abrupt increase in the output voltage (as a consequence of a purely capacitive way from the current generator to the electrodes), followed by a mono- or bipolar relaxation process: As long as the capacity of the double layer was kept constant, the voltage transient on the electrodes followed a monotonic decay, in line with the results of [12]. If, however, the capacity of the double layer was assumed to increase with the characteristic response time of the double layer, the shape of the voltage transient at the measuring electrodes could decently reproduce the bipolar character of the measured traces (Fig. 5). (Note that this feature was maintained within a wide range of scaling the capacitance of the double-layer, as long as C_{dl} did not exceed C_m more than a factor of 5 (Fig.S8), implying also that the permittivity inside the double layer should be closer to that of the membrane than to that of the bulk, being the latter corresponding to a C_{dl}/C_m ratio of more than 10.).

Hence, we can safely state that our hypothesis is capable to explain, at least qualitatively, all the five characteristic points found in the experiments. Nevertheless, more measurements are needed for a detailed molecular interpretation of the results. There are some possible reasons that may account for the voltage-dependence of the diffuse double-layer capacity, which go beyond the Gouy-Chapman model, such as.

- dipole potential changes due to water-reorientation at the membrane/electrolyte interface [16,23,24],
- changes of the dielectric constant within the double layer [25], or
- volume changes of the interfacial membrane components due to electrostriction effects [26].

Growing amount of new experimental and theoretical studies call the attention to the importance of the above factors in shaping the structure and dynamics of charged solid- electrolyte interfaces. For example, next-generation non-linear optical methods, such as heterodyne-detected second-harmonic generation (HD-SHG) spectroscopy, are able to give estimates to two important structural parameters of electric double layers: the total surface potential (Φ_{tot}) and the second-order nonlinear susceptibility ($\chi^{(2)}$) [27–30]. Experiments at solid-electrolyte interfaces revealed that dipole and multipolar contributions are included in these quantities, and hence, in the measurements of the differential capacity of the electric double layer, as well [28,30,31]. An abrupt charge displacement inside the membrane-embedded bR molecule, therefore, is expected to influence the surface potential and the dipole potential of the membrane, as well as the related differential capacitance of the double layer, both in a direct and indirect manner.

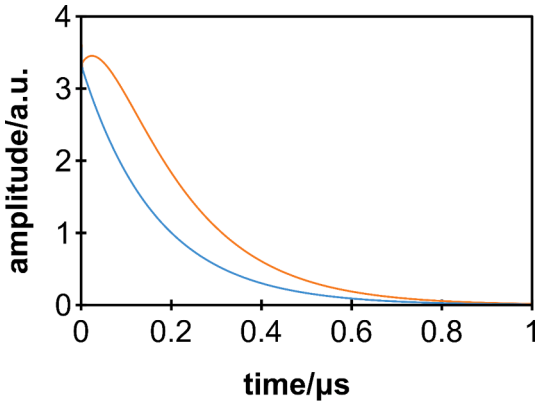

Fig. 5. Simulation of the fast voltage signal of bR, detectable by the measuring electrodes, using a substitution circuit modelling the electric response of a membrane-fragment - coupled ion pump - electrolyte system (Fig. S7) to an abrupt charge displacement in the pump protein (reversed sign). The capacity of the diffuse double layer kept constant, or increasing with the time constant of the rearrangement of the double layer (blue and red lines, respectively). (For more details, see Fig. S7).

In addition, the capacitance of the double layer should also explicitly depend on the relative dielectric permittivity (ε) of the double layer, according to Eqs. (1) and (2). Some recent estimates from various sets of experiments and computations ([25], and references therein) reveal that near the surface ε can be as low as ca. 2, mostly attributable to the oriented water molecules in the Stern layer, which are also the main source of non-vanishing $\chi^{(2)}$ of the interface, inevitable for the SHG experiments [28]. According to recent vibrational sum-frequency-generation (VSFG) experiments, surface dipoles induce orientation of polar liquid molecules [32], such as those of the solvent water [33]. Hence, intramolecular charge displacement – induced dipole potential changes should, in turn, affect the dielectric permittivity of the electric double layer.

The orientation of water molecules in the Stern layer, as a determinant of polarizability of the electric double layer, theoretically gives rise to an enhanced tendency for electrostriction, as well [34]. A similar effect has, in fact, been demonstrated experimentally, in the case of oriented water molecules confined in nanopores [35]. As a corollary, volume changes induced by the light-induced charge separation in bR, cannot be excluded, either.

Based on our experimental results, we cannot firmly make a preference for a single one from the above alternatives, but, given their interrelationship, all of them may contribute to the observed effects. However, independently from the exact molecular scenario, the assumption of a nonlinear behaviour of the membrane – double-layer system seems to be inevitable. This conclusion may be of interest in systems of electrified membrane interfaces in general, where the dynamics of the diffuse double layer plays a function-determining role [17]. In particular, the question arises whether the phenomenon of changing the double layer capacity followed by an abrupt electric dipole moment change in the membrane can play any physiological role. It is well known that all cells, notably, e.g., nerve cells [36], and subcellular units (such as mitochondria [37,38], chloroplasts [39]) have membranes in ionic environment, so the universality of the effect is straightforward, because the membranes surely have double layer around them in solutions. If the inserted proteins' charges move during basic physiological processes coupled to biological signal- or energy-transduction phenomena, these motions inevitably induce alterations in the double layers, which may have considerable physiological impact, amongst others, on cell–cell interactions [40], electro-mechanical coupling in skeletal muscle [41], or drug action (for a comprehensive review, see [42]). We assume that the biggest effects of surface potential changes should be expected in case of membrane potentials of excitable cells close to the threshold. In fact, Guttman and Barnhill established a repetitive firing of giant squid axon if the surface potential drops by as little as 8 mV [43].

In order to overcome the known limitations of the Hodgkin-Huxley model that does not consider, e.g., surface charge adsorption [44], or the reversible release and reabsorption of heat during firing, an exciting new paradigm has been raised to give an alternative description of nerve pulse propagation, based on nonlinear electromechanical waves (solitons) [26], where it is hypothesized that the action potential is the result of polarization and capacity changes of the nerve cell membrane [1]. In this context, the observed transient changes of the double-layer capacity may be of primary interest.

5. Summary:

We established for the first time that a nonlinear effect at the membrane-electrolyte interface has to be assumed to interpret the electric signals observed accompanying abrupt charge displacements inside the membrane. Based on the temperature dependence of the electric signals, the phenomena were interpreted as a consequence of voltage-induced changes in the double-layer capacity. General physiological implications of this finding are discussed.

Declaration of Competing Interest

The authors declare the following financial interests/personal relationships which may be considered as potential competing interests: Andras Der reports financial support was provided by National Research, Development and Innovation Office, Hungary.

Acknowledgements

This work was supported by grants of the National Research, Development and Innovation Office, Hungary (NKFI-1 K-124922), and the Eötvös Loránd Research Network (ELKH KÖ-36/2021).

Appendix A. Supplementary material

Supplementary data to this article can be found online at https://doi.org/10.1016/j.bioelechem.2022.108138.

References

[1] T. Heimburg, Comment on Tamagawa and Ikeda's reinterpretation of the Goldman–Hodgkin–Katz equation, Eur. Biophys. J. 47 (8) (2018) 865–867.
[2] L. Keszthelyi, P. Ormos, Electric signals associated with the photocycle of bacteriorhodopsin, FEBS Lett. 109 (2) (1980) 189–193.
[3] A. Dér, L. Keszthelyi, Charge motion during the photocycle of bacteriorhodopsin, Biochem. Mosc. 66 (11) (2001) 1234–1248.
[4] A. Dér, P. Hargittai, J. Simon, Time-resolved photoelectric and absorption signals from oriented purple membranes immobilized in gel, J. Biochem. Biophys. Methods 10 (5) (Mar. 1985) 295–300, https://doi.org/10.1016/0165-022X(85)90063-6.
[5] A.K. Dioumaev, D.S. Chernavskii, P. Ormos, G. Váró, L. Keszthelyi, Kinetics of the fast electric signal from oriented purple membrane, Biophys. J. 61 (5) (1992) 1194–1200.
[6] G.I. Groma, G. Szabo, G. Varo, Direct measurement of picosecond charge separation in bacteriorhodopsin, Nature 308 (5959) (1984) 557–558.
[7] G.I. Groma, J. Hebling, C. Ludwig, J. Kuhl, Charge displacement in bacteriorhodopsin during the forward and reverse bR-K phototransition, Biophys. J. 69 (5) (1995) 2060–2065.
[8] L. Oroszi, A. Der, P. Ormos, Theory of electric signals of membrane proteins in three dimensions, Eur. Biophys. J. 31 (2) (2002) 136–144.
[9] K. Barabás, A. Dér, Z. Dancsházy, P. Ormos, L. Keszthelyi, M. Marden, Electro-optical measurements on aqueous suspension of purple membrane from Halobacterium halobium, Biophys. J. 43 (1) (Jul. 1983) 5–11, https://doi.org/10.1016/S0006-3495(83)84317-3.
[10] A. Dér, L. Oroszi, Á. Kulcsár, L. Zimányi, R. Tóth-Boconádi, L. Keszthelyi, W. Stoeckenius, P. Ormos, Interpretation of the spatial charge displacements in bacteriorhodopsin in terms of structural changes during the photocycle, Proc. Natl. Acad. Sci. 96 (6) (1999) 2776–2781, https://doi.org/10.1073/pnas.96.6.2776.
[11] C. D. Hodgman and M. Frankel, "Handbook of chemistry and physics," 1960.
[12] L. Oroszi, O. Hasemann, E. Wolff, A. Dér, Modeling of ionic relaxation around a biomembrane disk, Bioelectrochemistry 60 (1-2) (2003) 97–106.
[13] P. Joliot, R. Delosme, Flash-induced 519 nm absorption change in green algae, Biochim. Biophys. Acta BBA-Bioenerg. 357 (2) (1974) 267–284.
[14] L. Zimányi, G. Garab, Configuration of the light induced electric field in thylakoid and its possible role in the kinetics of the 515 nm absorbance chance, J. Theor. Biol. 95 (4) (1982) 811–821.
[15] M.R. Moncelli, L. Becucci, R. Guidelli, The intrinsic pKa values for phosphatidylcholine, phosphatidylethanolamine, and phosphatidylserine in monolayers deposited on mercury electrodes, Biophys. J. 66 (6) (1994) 1969–1980.
[16] M.R. Moncelli, L. Becucci, F.T. Buoninsegni, R. Guidelli, Surface dipole potential at the interface between water and self-assembled monolayers of phosphatidylserine and phosphatidic acid, Biophys. J. 74 (5) (1998) 2388–2397.
[17] A.A. Moya, Theory of the formation of the electric double layer at the ion exchange membrane–solution interface, Phys. Chem. Chem. Phys. 17 (7) (2015) 5207–5218, https://doi.org/10.1039/C4CP05702C.
[18] A. Chrambach and D. Rodbard, "Polyacrylamide Gel Electrophoresis," p. 13.
[19] L.P. Yezek, H.P. van Leeuwen, An electrokinetic characterization of low charge density cross-linked polyacrylamide gels, J. Colloid Interface Sci. 278 (1) (Oct. 2004) 243–250, https://doi.org/10.1016/j.jcis.2004.05.026.
[20] A. Dolfi, F. Tadini-Buoninsegni, M.R. Moncelli, R. Guidelli, Photocurrents generated by bacteriorhodopsin adsorbed on thiol/lipid bilayers supported by mercury, Langmuir 18 (16) (2002) 6345–6355.
[21] H.-W. Trissl, A. Der, P. Ormos, L. Keszthelyi, Influence of stray capacitance and sample resistance on the kinetics of fast photovoltages from oriented purple membranes, Biochim. Biophys. Acta BBA - Bioenerg. 765 (3) (Jun. 1984) 288–294, https://doi.org/10.1016/0005-2728(84)90168-3.
[22] T. Heimburg, Phase Transitions in Biological Membranes, in: C. Demetzos, N. Pippa (Eds.), Thermodynamics and Biophysics of Biomedical Nanosystems, Springer Singapore, Singapore, 2019, pp. 39–61, https://doi.org/10.1007/978-981-13-0989-2_3.
[23] R.J. Clarke, C. Lüpfert, Influence of anions and cations on the dipole potential of phosphatidylcholine vesicles: a basis for the Hofmeister effect, Biophys. J. 76 (5) (1999) 2614–2624.
[24] L. Wang, Measurements and implications of the membrane dipole potential, Annu. Rev. Biochem. 81 (1) (2012) 615–635.
[25] M.D. Boamah, P.E. Ohno, F.M. Geiger, K.B. Eisenthal, Relative permittivity in the electrical double layer from nonlinear optics, J. Chem. Phys. 148 (22) (2018) 222808, https://doi.org/10.1063/1.5011977.
[26] T. Heimburg, A.D. Jackson, On soliton propagation in biomembranes and nerves, Proc. Natl. Acad. Sci. 102 (28) (2005) 9790–9795.
[27] B. Rehl *et al.*, "Water Dipole Populations in the Electrical Double Layer and Their Contributions to the Total Interfacial Potential at Different Surface Charge Densities," Chemistry, preprint, Feb. 2022. doi: 10.26434/chemrxiv-2022-p5fwp.
[28] M.D. Boamah, P.E. Ohno, E. Lozier, J. Van Ardenne, F.M. Geiger, Specifics about Specific Ion Adsorption from Heterodyne-Detected Second Harmonic Generation, J. Phys. Chem. B 123 (27) (2019) 5848–5856, https://doi.org/10.1021/acs.jpcb.9b0442510.1021/acs.jpcb.9b04425.s001.
[29] E. Ma, P.E. Ohno, J. Kim, Y. Liu, E.H. Lozier, T.F. Miller, H.-F. Wang, F.M. Geiger, A New Imaginary Term in the Second-Order Nonlinear Susceptibility from Charged Interfaces, J. Phys. Chem. Lett. 12 (24) (2021) 5649–5659, https://doi.org/10.1021/acs.jpclett.1c0110310.1021/acs.jpclett.1c01103.s001.
[30] E. Ma, J. Kim, HanByul Chang, P.E. Ohno, R.J. Jodts, T.F. Miller, F.M. Geiger, Stern and Diffuse Layer Interactions during Ionic Strength Cycling, J. Phys. Chem. C 125 (32) (2021) 18002–18014, https://doi.org/10.1021/acs.jpcc.1c0483610.1021/acs.jpcc.1c04836.s001.
[31] C.C. Doyle, Y.u. Shi, T.L. Beck, The Importance of the Water Molecular Quadrupole for Estimating Interfacial Potential Shifts Acting on Ions Near the Liquid-Vapor Interface, J. Phys. Chem. B 123 (15) (2019) 3348–3358, https://doi.org/10.1021/acs.jpcb.9b0128910.1021/acs.jpcb.9b01289.s001.
[32] D. Rodriguez, M.D. Marquez, O. Zenasni, L.T. Han, S. Baldelli, T.R. Lee, Surface Dipoles Induce Uniform Orientation in Contacting Polar Liquids, Chem. Mater. 32 (18) (2020) 7832–7841, https://doi.org/10.1021/acs.chemmater.0c02471.
[33] F. Yesudas, M. Mero, J. Kneipp, Z. Heiner, High-resolution and high-repetition-rate vibrational sum-frequency generation spectroscopy of one- and two-component phosphatidylcholine monolayers, Anal. Bioanal. Chem. 411 (19) (Jul. 2019) 4861–4871, https://doi.org/10.1007/s00216-019-01690-9.
[34] V. Sundar, R.E. Newnham, Electrostriction and polarization, Ferroelectrics 135 (1) (Oct. 1992) 431–446, https://doi.org/10.1080/00150199208230043.
[35] D. Vanzo, D. Bratko, A. Luzar, Nanoconfined water under electric field at constant chemical potential undergoes electrostriction, J. Chem. Phys. 140 (7) (2014) 074710, https://doi.org/10.1063/1.4865126.
[36] D.E. Goldman, Potential, impedance, and rectification in membranes, J. Gen. Physiol. 27 (1) (1943) 37–60.
[37] H. Pauly, L. Packer, The relationship of internal conductance and membrane capacity to mitochondrial volume, J. Cell Biol. 7 (4) (1960) 603–612.
[38] F. Scholkmann, Long range physical cell-to-cell signalling via mitochondria inside membrane nanotubes: a hypothesis, Theor. Biol. Med. Model. 13 (1) (2016) 1–22.
[39] O. Zsiros, R. Ünnep, G. Nagy, L. Almásy, R. Patai, N.K. Székely, J. Kohlbrecher, G. Garab, A. Dér, L. Kovács, Role of protein-water interface in the stacking interactions of granum thylakoid membranes—As revealed by the effects of Hofmeister salts, Front. Plant Sci. 11 (2020), https://doi.org/10.3389/fpls.2020.01257.
[40] B.W. Ninham, V.A. Parsegian, Electrostatic potential between surfaces bearing ionizable groups in ionic equilibrium with physiologic saline solution, J. Theor. Biol. 31 (3) (1971) 405–428.
[41] M. Dörrscheidt-Käfer, The action of D600 on frog skeletal muscle: facilitation of excitation-contraction coupling, Pflüg. Arch. 369 (3) (1977) 259–267.
[42] D.L. Gilbert, G. Ehrenstein, Membrane surface charge, Curr. Top. Membr. Transp. 22 (1984) 407–421.
[43] R. Guttman, R. Barnhill, Oscillation and Repetitive Firing in Squid Axons: Comparison of experiments with computations, J. Gen. Physiol. 55 (1) (1970) 104–118.
[44] H. Tamagawa, K. Ikeda, Another interpretation of the Goldman–Hodgkin–Katz equation based on Ling's adsorption theory, Eur. Biophys. J. 47 (8) (2018) 869–879.